Jérémie V.

DEVELOPMENT AND EVALUATION OF EQUIVALENT-FLUID APPROXIMATIONS FOR SEA-BOTTOM SOUND REFLECTION

Jing-Fang Li [a] **and Murray Hodgson** [b]

[a] Department of Mechanical Engineering, University of British Columbia
2324 Main Mall, Vancouver, B.C., Canada V6T 1Z4

[b] Occupational Hygiene Programme and Department of Mechanical Engineering
University of British Columbia, 2206 East Mall, Vancouver, B.C., Canada V6T 1Z3

ABSTRACT

Almost all marine sediments possess enough rigidity to transmit shear waves. Shear waves are important in underwater sound propagation because compressional waves can be partially converted to shear waves or Stoneley waves at reflection boundaries. An equivalent-seabed model is an approximate method to simplify the mathematical analysis and reduce the calculational expense in modelling water-borne shallow-water sound propagation, taking seabed shear-wave effects into account. According to this method, the seabed with rigidity is treated as an equivalent fluid. However, seabed shear-wave effects are included in the adjustable parameters of the equivalent fluid. The objective of this work was to develop and evaluate equivalent-fluid seabed models. Existing equivalent-fluid seabeds have been evaluated by calculating the reflection coefficient of the bottom. Meanwhile, shear-wave effects on reflection and on the total impedance of seabeds have been studied. A new effective-seabed model is proposed from the calculation of the effective impedance of the seabed. Comparison of the new model with the existing model shows that the new model agrees better with the solid seabed at low grazing angles. Furthermore, grazing-angle-dependent parameters of the equivalent-fluid seabed are proposed.

RESUME

La réflexion du son sur le fond de mer est très importante dans des études de la propagation acoustique sous-marine. Comme la rigidité de la plupart des fonds permet la propagation des ondes de compression et de cisaillement, le probème de la détermination de l'amplitude et de la phase du coefficient de réflexion devient plus compliqué et les effets dûs à la propagation de ces ondes ne peuvent être négligés. Une méthode approchée consiste à remplacer le fond solide par un "fluide équivalent" en faisant un choix des paramètres qui prennent en compte l'effet des ondes de compression et de cisaillement. L'objet de ce travail est d'évaluer et de developper les modèles de fluides équivalents de la littérature en les utilisant pour calculer le coefficient de réflexion du fond. Les effets des ondes de cisaillement sont analysés. Un nouveau modèle de fluide equivalent ("fond effectif") est proposé à partir de l'expression de l'impédance effective du fond. La comparaison entre ce nouveau modèle et les modèles existants montre que celui-ci fournit une meilleure prédiction du coefficient de refléxion. On propose egalement un modèle qui comporte des paramètres permettant de prendre en compte les effets de l'incidence rasante. Il est montré que l'utilisation de ces paramètres donne un meilleur agrément avec les valeurs des fonds marins réels pour la prévision de leurs coefficients de réflexion.

1. INTRODUCTION

Sound reflection from the seabed is very important in the study of sound propagation in shallow water. As most seabeds support both compressional and shear waves, seabed rigidity affects the reflection loss and phase shift of the bottom reflection [1]. In this case, the problem of modelling sound reflection from the seabed becomes more complicated. An approximate method is to replace the solid with a fluid by choosing suitable seabed parameters. This replacement fluid is termed the equivalent-fluid seabed. An equivalent-seabed model is an approximate method to simplify the mathematical analysis and reduce the calculational expense in modelling water-borne shallow-water sound propagation, taking seabed shear-wave effects into account.

Effective-seabed models have been developed by several authors. Bucker [2] described a systematic technique for generating an equivalent bottom for use with the split-step algorithm. In Bucker's model, the equivalent bottom is a set of absorbing liquid-sediment layers. Tappert [3] described a technique to replace the solid seabed by an equivalent-fluid seabed with additional attenuation due to the shear wave. This treatment allows the continued use of a layered fluid-sediment geoacoustic bottom model as contained in the standard PE propagation model. Williams and Eby [4] noticed that the effects of shear waves on the phase speed are roughly equivalent to that of decreasing the density of the sea bed. Frisk and Lynch [5] used this idea to model the effect of shear waves, and obtained the reduced density. Tindle and Zhang [6] developed an equivalent-fluid model for a low-shear sea bottom and gave an equivalent seabed with real parameters. Then they developed a complex-density model [7].

The objective of the work reported here was to develop and evaluate equivalent-fluid seabed models. First, shear-wave effects on the reflection coefficient and the total impedance of the seabed have been studied. Second, existing effective-seabed models are examined and evaluated numerically in the second section. Then a new effective-seabed model is proposed from the calculation of the effective impedance of the seabed. Comparison of the new model with the existing model shows that the new model agrees better with the solid seabed. Furthermore, grazing-angle-dependent parameters of the equivalent-fluid seabed are proposed. It is shown that one can obtain better prediction of the reflection coefficient of the equivalent fluid by adjusting the grazing angle in the parameters of the equivalent fluid.

2. EFFECTS OF SHEAR WAVES

The equivalent-fluid seabed can be derived from the calculation of the reflection coefficient at fluid and solid interfaces [3, 6, 7]. In this section the reflection coefficient of the bottom is given. Then the shear-wave effects are studied using the expression for the reflection coefficient. This study will guide the modelling of the equivalent-fluid seabed.

2.1 Reflection Coefficient of the Bottom

Consider the case of homogeneous water of density ρ_1 and sound speed c_1 lying over a homogeneous seabed of density ρ_2, compressional- and shear-wave speeds c_p and c_s, and attenuation coefficients of the compressional and shear waves α_p and α_s (in dB/wavelength), respectively. The attenuation in the water is neglected. The bottom reflection coefficient is written as [10]:

$$ R_{fs} = \frac{Z_b - Z_1}{Z_b + Z_1}, \qquad (1) $$

where $Z_1 = \rho_1 c_1 / \sin \theta_1$ is the normal impedance of the fluid. $Z_b = Z_p \sin^2 2\theta_s + Z_s \cos^2 2\theta_s$ is the total impedance of the bottom. $Z_p = \rho_2 \hat{C}_p / \sin \theta_p$ and $Z_s = \rho_2 \hat{C}_s / \sin \theta_s$ are the impedances of the compressional and shear waves in the bottom, respectively. θ_1 is the grazing angle. θ_p and θ_s are the refraction angles of the compressional and shear waves, respectively. $\hat{C}_p$ and $\hat{C}_s$ are the complex sound speeds of the compressional and shear waves. If the attenuation coefficients α_p and α_s (in dB/wavelength) are used, $\hat{C}_p$ and $\hat{C}_s$ are expressed, respectively, as:

$$ \hat{C}_p = c_p/(1 + i\xi\alpha_p), \qquad \hat{C}_s = c_s/(1 + i\xi\alpha_s), \qquad (2) $$

where $\xi = 1/(40\pi\log_{10}e)$, $e = 2.7183$. Snell's law at the fluid/solid interface is:

$$ \frac{c_1}{\cos \theta_1} = \frac{\hat{C}_p}{\cos \theta_p} = \frac{\hat{C}_s}{\cos \theta_s}. \qquad (3) $$

By the use of Snell's law at the fluid/solid interface, the reflection coefficient of the bottom can be written in the following form:

$$ R_{fs} = \frac{\rho_2 \hat{C}_p P(\theta_1)/ \sin \theta_p - \rho_1 c_1 / \sin \theta_1}{\rho_2 \hat{C}_p P(\theta_1)/ \sin \theta_p + \rho_1 c_1 / \sin \theta_1}, \qquad (4) $$

where $P(\theta_1)$ is the shear-wave factor, written as:

$$ P(\theta_1) = \cos^2 2\theta_s + 4\frac{\hat{C}_s}{\hat{C}_p} \sin \theta_s \cos^2 \theta_s \sin \theta_p $$
$$ = (1 - 2\frac{\hat{C}_s^2}{c^2})^2 + i4\frac{\hat{C}_s^3}{c^3}\sqrt{1 - c^2/\hat{C}_p^2}\sqrt{1 - \hat{C}_s^2/c^2}, \qquad (5) $$

with $c = c_1/ \cos \theta_1$. The shear-wave factor $P(\theta_1)$ represents shear-wave effects in the bottom. It is obviously that when $c_s = 0$, $P = 1$ and that at normal incidence, $\theta_1 = \pi/2$, $P = 1$.

The normal impedance at the interface relating to the shear-wave factor is thus given by:

$$ Z_b = \rho_2 \hat{C}_p P(\theta_1)/ \sin \theta_p = \frac{\rho_2 \hat{C}_p P(\theta_1)}{\sqrt{1 - \hat{C}_p^2/c^2}}. \qquad (6) $$

Table 1 shows data sets of typical seabed parameters. The reference from which the data was taken is indicated beside the data-set designation. Fig. 1 shows the effects seabed attenuation and rigidity on the reflection coefficient for data sets B and E. It is shown that: (i) When c_s is small (see seabed B, for example), there is no big difference between the bottom loss due to the compressional-wave attenuation and that due to the shear waves. Thus, the bottom losses due to the excitation of

Table 1. – Data sets of typical seabed parameters

DATA SET	ρ_2/ρ_1	c_1 (m/s)	c_p (m/s)	c_s (m/s)	α_p (dB/λ_p)	α_s (dB/λ_s)
A[7]	1.5	1508.7	1605	340	0.1814	6.8
B[7]	1.9	1500.0	2000	450	0.4	0.225
C[6]	2.0	1509.0	1750	600	0.6	1.5
D[8]	2.0	1500.0	2150	650	0.32	0.2
E[9]	2.2	1500.0	2250	1000	0.4	1.0

low-speed shear waves can be simulated by a fluid with increased attenuation of the bottom [3]; (ii) When c_s is large (see seabed E), the bottom losses are mainly due to the excitation of the shear waves. One cannot obtain the bottom loss of a solid seabed by increasing the attenuation without taking account of the shear waves; (iii) The excitation of shear waves in the seabed causes large reflection losses, because of the transformation of the water-borne energy into the energy of shear-wave propagation in the seabed; (iv) Phase shift of the reflection occurs when the grazing angle θ_1 is less than

the critical angle $\theta_c = \cos^{-1} c_1/c_p$. This means that the reflection coefficient depends strongly on the grazing angle at $\theta_1 < \theta_c$.

2.2 Total Impedance of the Seabed

The total impedance of the seabed was calculated using Eq. (6) for data sets B and E. The impedance with shear waves neglected was also calculated. The results are shown in Fig. 2. The comparisons between the exact impedance and that without shear waves show that: (i) The excitation of shear waves in the seabed causes a decrease of the amplitude of the total impedance of the seabed; (ii) The phase shift of the total impedance occurs when $\theta_1 < \theta_c = \cos^{-1} c_1/c_p$; (iii) When c_s is large, the decrease and phase shift of the total impedance of the seabed become very large. The maximum decrease in magnitude and phase shift occur at the critical grazing angle θ_c; (iv) At low grazing angle it may be possible to treat a solid bottom with a low shear-wave speed as a fluid by decreasing the total impedance of the bottom [4, 5].
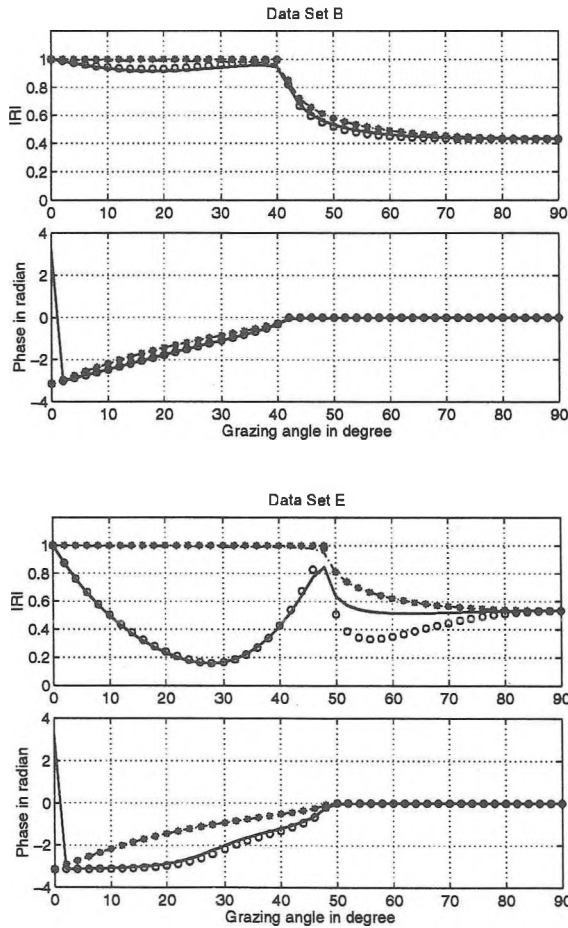

Figure 1. – Reflection coefficient versus grazing angle for data sets B and E using Eq. (1). (———) solid seabed with shear attenuations; ($\ast\ast\ast$) $c_s = 0$, $\alpha_p = 0$ and $\alpha_s = 0$; ($.-.-.-.-$) $c_s = 0$ and $\alpha_s = 0$, $\alpha_p \neq 0$; ($\circ\circ\circ$) $c_s \neq 0$, $\alpha_p = 0$ and $\alpha_s = 0$.
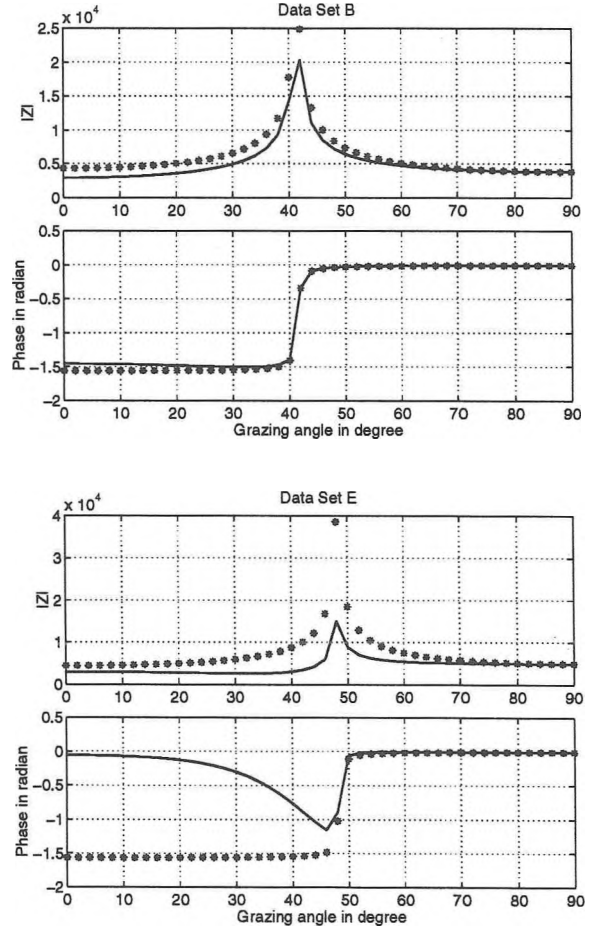

Figure 2. – Bottom impedance versus grazing angle for data sets B and E: (———) solid seabed with shear waves; ($\ast\ast\ast$) without shear waves.

3. EVALUATION OF EXISTING EFFECTIVE-SEABED MODELS

An equivalent-seabed model is an approximate method to simplify the mathematical analysis and reduce the calculational expense in modelling water-borne shallow-water sound propagation, taking seabed shear-wave effects into account. According to this method, the seabed with rigidity is treated as an equivalent fluid. However, seabed shear-wave effects which cannot be neglected are included in the adjustable parameters of the equivalent fluid, such as the density and the attenuation, which are related to the geoacoustic parameters of the solid seabed.

Three methods were considered in the early studies of the effective seabeds, considering the effects of shear waves in seabed on the sound field in shallow water: (i) Regard the excitation of low-speed shear waves as a loss mechanism and model this effect by increased attenuation parameters [2, 3, 13, 14]. For example, Ingenito and Wolf [13] modelled normal-mode attenuation in shallow water over a consolidated bottom by assuming a fluid bottom and adjusting the boundary condition to allow for attenuation due to shear-wave losses. This method was used by Jensen and Kuperman [9] to include the effect of low-velocity shear waves on propagation in the modal computation. Tunnel and Tango [14] modelled the shear-wave effects by increasing the bottom attenuation. They computed the plane-wave reflection coefficients for multilayered bottoms; the bottom loss from a shear-supporting bottom was matched with that from a bottom with no shear waves but with a compressional-wave attenuation increased by a factor of 1.25. However, when the mode number exceeded 5, the overall transmission-loss levels were well reproduced, but not the phase features. Tappert [3] derived a formula for the effective attenuation coefficient of a seabed. He treated a solid seabed as a fluid sediment, the attenuation of which was replaced by an additional attenuation caused by shear waves; (ii) A slow viscoelastic solid seabed is roughly equivalent to a fluid seabed of reduced density [4]. Seabed rigidity also decreases the bottom impedance and increases the phase shift associated with each bottom bounce. Williams and Eby [4] considered mode propagation over a viscoelastic solid seabed and noted that, as far as mode phase speeds are concerned, a slow viscoelastic solid seabed is roughly equivalent to a fluid seabed of reduced density. This result was used by Frisk and Lynch [5] to model the effect of shear waves; (iii) Thick unconsolidated sediments that support shear waves can be modelled as equivalent seabeds with adjusted parameters [6, 7].

In this section, the existing equivalent-fluid-seabed models will be reviewed and evaluated, including Tappert's model [3], Frisk and Lynch's model [5] and Tindle and Zhang's models [6, 7].

3.1 Tappert's Model [3]

Tappert derived a simple technique for including in the PE model the loss due to conversion of compressional waves into shear waves at the water/bottom interface. In this technique, the conversion of compressional waves into shear waves can be treated simply as a loss mechanism when modelling the propagation of sound waves in shallow water at frequencies above approximately 10 Hz. Thus the effects of shear waves are included by calculating the additional loss due to shear-wave conversion. By the use of this technique, the solid bottom supporting shear waves can be replaced by a layered-fluid sediment geoacoustical bottom model as contained in the standard PE propagation model.

The additional loss due to shear waves in the bottom is obtained by comparing the amplitude of the reflection coefficient R_{ff} at an interface between a low-loss fluid and a lossy fluid and that at an interface between a low-loss fluid and a low-loss elastic solid R_{fs}. This comparison is based on the mathematical approximation to the reflection coefficient with the following hypotheses: (i) $c_p > c_1$; (ii) $\theta_1 << \theta_c = \cos^{-1} c_1/c_p$; (iii) $\alpha_p << \omega/c_p$; (iv) $c_s << c_1 < c_p$. Then the loss for the effective fluid is given by:

$$\alpha_e = \alpha_p + \frac{4}{\xi}\frac{\sin^3\theta_c}{\cos^2\theta_c}\left(\frac{c_s}{c_1}\right)^3, \qquad (7)$$

where $\cos\theta_c = c_1/c_p$, $\sin\theta_c = \sqrt{1-(c_1/c_p)^2}$. If the bottom is lossy, complex sound speeds of the compressional and shear waves $\hat{C}_p$ and C_s are used. Then the attenuation coefficient becomes complex. However, $\text{Im}\{\alpha_e\} << \text{Re}\{\alpha_e\}$, $\alpha_e \approx \text{Re}\{\alpha_e\}$. For small angles of incidence, the loss due to shear-wave conversion may be simulated by means of a fluid bottom by adding to the volume loss of the effective-fluid bottom. An effective-fluid bottom with loss α_e given by Eq. (7) will cause the same reflection loss to plane waves incident at small angles as a lossy elastic bottom. The reflection coefficient at the interface of the fluid and the bottom is calculated using Tappert's model for data set C. The results are shown in Fig. 3.

3.2 Model of Reduced Density [4, 5]

Williams and Eby [4] noticed that the effects of shear waves on the phase speed are roughly equivalent to that of decreasing the density contrast ρ_2/ρ_1. Frisk and Lynch [5] used this idea to model the effect of shear waves, and obtained the reduced density in the case of $c_s << c_1 < c_p$:

$$\rho_e = \rho_2(1-2r)^2, \quad \text{with} \quad r = c_s^2/c_1^2. \qquad (8)$$

The reflection coefficient using the reduced-density model is shown in Fig. 3 for data set C. The reflection coefficient at
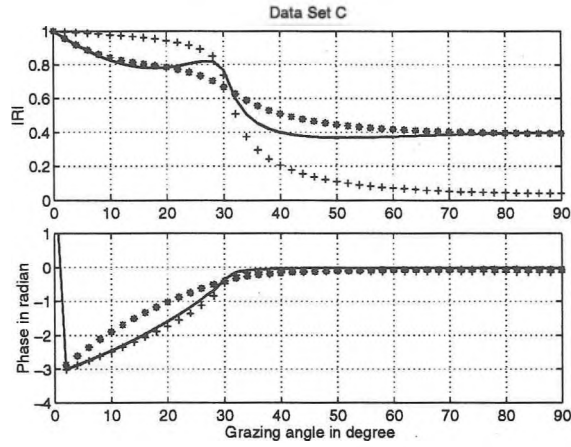
Figure 3 Amplitude and phase of the reflection coefficient for data set C. (———) solid seabed with shear waves; (* * *) Tappert's model; (+ + +) model of reduced impedance.

a fluid/solid interface with shear waves is also shown in Fig. 3. It is noted from the comparisons of the results shown in Fig. 3 that: (i) In the case of low shear-wave speed, the model of increased attenuation gives better results than the model of reduced impedance in the prediction of the amplitude of the reflection coefficient. This is because the attenuation coefficient Eq. (7) was derived when only the amplitude of the reflection coefficient was being considered. However, the model of reduced impedance gives better results than the model of increased attenuation in predicting the phase of the reflection coefficient; (ii) From the previous discussions, it can be concluded that shear waves in seabeds cause increased attenuation of the amplitude and phase shift of the reflection coefficient. The effects of the increased attenuation coefficient result in greater seabed losses, whereas the effect of the reduced impedance results in phase shifts of the reflection coefficient.

3.3 Tindle and Zhang's Models [6, 7]

The basic relationship used to derive Tindle and Zhang's two types of equivalent-fluid approximations is obtained by making the reflection coefficient at the fluid/solid interface equal to the reflection coefficient at the fluid/equivalent-fluid interface [6]:

$$\rho_e/\eta_e = \rho_2 P(\theta_1)/\eta_2, \qquad (9)$$

where

$$\eta_2 = i\frac{\omega}{\hat{C}_p}\sqrt{1 - \frac{\hat{C}_p^2}{c_1^2}\cos^2\theta_1}, \quad \eta_e = i\frac{\omega}{\hat{C}_e}\sqrt{1 - \frac{\hat{C}_e^2}{c_1^2}\cos^2\theta_1},$$

with $\hat{C}_e = c_e/(1 + i\xi\alpha_e)$. The equivalent-fluid parameters are the set of values of sound speed c_e, density ρ_e and attenuation coefficient α_e that gives the best approximation to the solid-seabed reflection coefficient. Three types of equivalent-

seabed models were obtained from the relationship (9) using the hypotheses $\alpha_p \ll \omega/c_p$ and $\alpha_s \ll \omega/c_s$.

The sound speed of the equivalent fluid for the three types is given by:

$$c_e = c_p, \qquad (10)$$

in order for the two bottom reflection coefficients to have the same critical angle and the same number of discrete normal modes in a waveguide.

Type 1: Equivalent Fluid with Real Parameters

The other two parameters are determined approximately from Eq. (9) using the hypotheses $\alpha_p \ll \omega/c_p$ and $\alpha_s \ll \omega/c_s$, expanding the terms in Eq. (9) and retaining only the terms of lower order, then equating real and imaginary parts in the resulting expansion.

The attenuation coefficient of the equivalent fluid with real parameters is given by:

$$\alpha_e = \alpha_p + \frac{8\alpha_s r(1-q)}{q(1-2r)} + \frac{4r^{3/2}(1-q)^{3/2}(1-r)^{1/2}}{\xi q(1-2r)^2}. \quad (11)$$

Tindle and Zhang gave two expressions for the density of the equivalent fluid. The first one is solved from Eq. (9) by taking the lowest order of the Taylor's expansion for Eq. (9):

$$\rho_e = \rho_2(1 - 2r)^2. \qquad (12)$$

This is the same expression as that in the model of reduced density (see Eq. (8)).

The second expression for the density is obtained when the first and the second terms of the Taylor's expansion of Eq. (9) are taken into account:

$$\rho_e = \rho_2(1 - 2r)^2 \frac{1 - s\alpha_p^2}{1 - s\alpha_e^2}, \qquad (13)$$

where $q = c_1^2/c_p^2$, $r = c_s^2/c_1^2$ and $s = \xi^2 q(1+2q)/[2(1-q)^2]$. When $s\alpha_p^2$ is much smaller than $s\alpha_e^2$:

$$\rho_e = \rho_2(1 - 2r)^2 \frac{1}{1 - s\alpha_e^2}. \qquad (14)$$

Table 2 gives attenuation coefficients of the equivalent fluid calculated using Eq. (11). The densities of the equivalent fluid calculated using Eqs. (12)-(14) for data sets A to E are also shown in Table 2. It is noted that $\alpha_e > \alpha_p$ for data sets A to E and that $\rho_e < \rho_2$ only for data sets A, B and C. Thus this model includes two ways to match the bottom losses caused by shear waves: increase of the attenuation and decrease of the density. As a result, the impedance of the seabed is decreased and the seabed becomes 'softer' because of the shear waves.

Comparison of the densities of the equivalent fluid obtained using Eqs. (12) - (14) shows that $\rho_e < \rho_2$ for data sets A,

DATA SET	ρ_e Eq. (12)	ρ_e Eq. (13)	ρ_e Eq. (13)	α_e Eq. (11)
A	1.2290	1.229	1.23	0.722
B	1.28	1.3097	1.3099	4.855
C	0.93	1.1455	1.1475	6.2607
D	0.78	2.0557	2.0558	31.8414
E	0.03	-4.3957e-06	-4.3960E-06	3.6787e+0.3

B and C. ρ_e estimated by Eq. (12) is less than that estimated by Eqs. (13) and (14). There is almost no difference between values calculated using Eqs. (13) and (14). This is because $s\alpha_p^2$ is so small in comparison with $s\alpha_e^2$ for all data sets used in this study that one can use Eq. (14), which is simpler than Eq. (13), to calculate ρ_e.

Now look at the results for data sets D and E. According to Table 2, the density of the equivalent fluid is larger than that of the solid for data set D, and is negative for data set E. In the
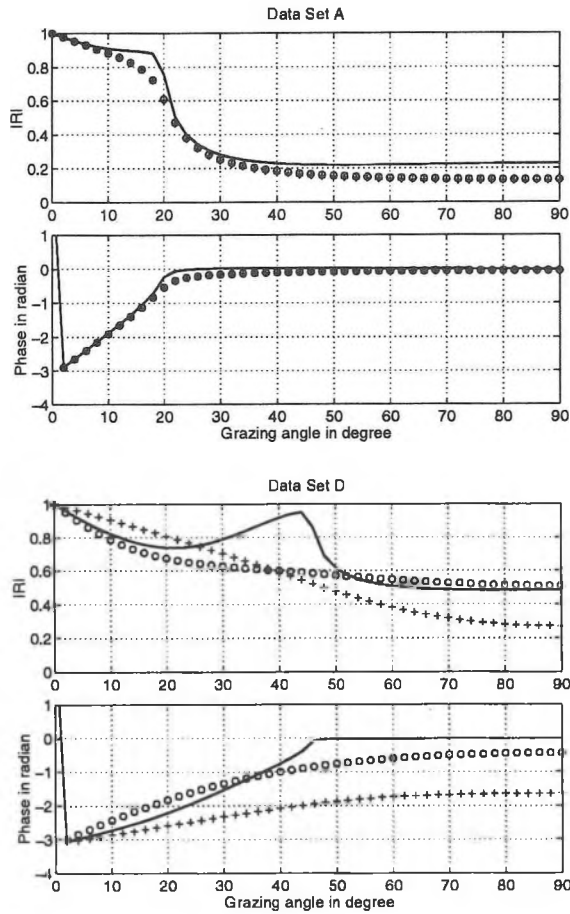

Data Set A

Data Set D

Figure 4 – Reflection coefficient versus grazing angle for data sets A and D. (——) solid seabed with shear waves; (+ + +) use of Eq. (12); (o o o) use of Eq. (14).

results, the impedance of the equivalent fluid bear no relation to that of the corresponding solid. From Eq. (9), it is noted that when $(c_s/c_1)^2 \approx 0.5$, $\alpha_s \to \infty$, resulting in $\rho_e < 0$. Therefore this model does not give the right density of the equivalent fluid and is not valid when the shear-wave speed is large.

Fig. 4 shows the reflection coefficient of the equivalent-fluid seabed calculated using the densities estimated by Eqs. (12) and (14) for data sets A and D. The sound speed and the attenuation coefficient of the equivalent-fluid seabed are calculated by Eqs. (10) and (11). It is noted that there are no significant differences between Eq. (12) and Eq. (14) for data set A for which the shear-wave sound speeds is $c_s = 340$. For data set D, Eq. (14) gives better estimation of the reflection coefficient than does Eq. (12).

In order to get a positive value for the density of the equivalent-fluid seabed using Eq. (14), we must have the following conditions:

$$\Gamma = s\alpha_e^2 < 0.5, \quad \text{and} \quad r << 0.5. \tag{15}$$

Γ was calculated for data sets A to E and is shown in Table 3. It is noted that $\Gamma < 0.5$ and $r << 0.5$ for data sets A, B, and C. Thus Eq. (11) gives a good estimation of α_e which then can be used to estimate the density of the equivalent-fluid seabed ρ_e using Eq. (12) or Eq. (14). For data set E, $\Gamma >> 1$ and $r \approx 0.5$. Thus, Eqs. (11) and (14) do not give good estimates of the attenuation coefficient and the density of the equivalent fluid.

Type 2: Equivalent Fluid with Complex Density

Using Eq. (9), Zhang and Tindle developed the complex-density model. The parameters of the equivalent seabed are given as follows:

Attenuation coefficient:

$$\alpha_e = \alpha_p. \tag{16}$$

Complex density:

$$\rho_e = \rho_2 P(\theta_1)|_{\theta_1=0}. \tag{17}$$

As $|P(0)| < 1$ when $c_s \neq 0$, the density of the equivalent fluid ρ_e is less than that of the seabed ρ_2. As a result, the impedance of the equivalent fluid decreases. Thus reflection

Table 3. Criteria of Γ of Tindle and Zhang's Type 1.

DATA	$q = (c_1/c_p)^2$	$r = (c_s/c_1)^2$	Γ
A	0.8836	0.0508	0.0158
B	0.5625	0.0900	0.0247
C	0.7435	0.1581	0.1850
D	0.4867	0.1878	0.6206
E	0.4444	0.4444	6179.4

losses of the equivalent fluid could match the reflection losses of the solid seabed with shear waves.

Fig. 5 shows the amplitudes and phases of the reflection coefficients of the solid and the equivalent fluids with real parameters, and of the complex density, for data sets A and E. It is noted that the equivalent fluid with real parameters is a good approximation at low grazing angle for data set A. For data set E where the shear-wave speed is large, the equivalent fluid with real parameters gives wrong results in the estimation of the reflection coefficient. However, the equivalent fluid of complex density gives better approximations to the exact values than the equivalent fluid with real parameters, even when the shear-wave speed is large. This is because Eq. (16) is not restricted to the small attenuations. However, this model is only valid for low grazing angles when the shear-wave speed becomes larger.
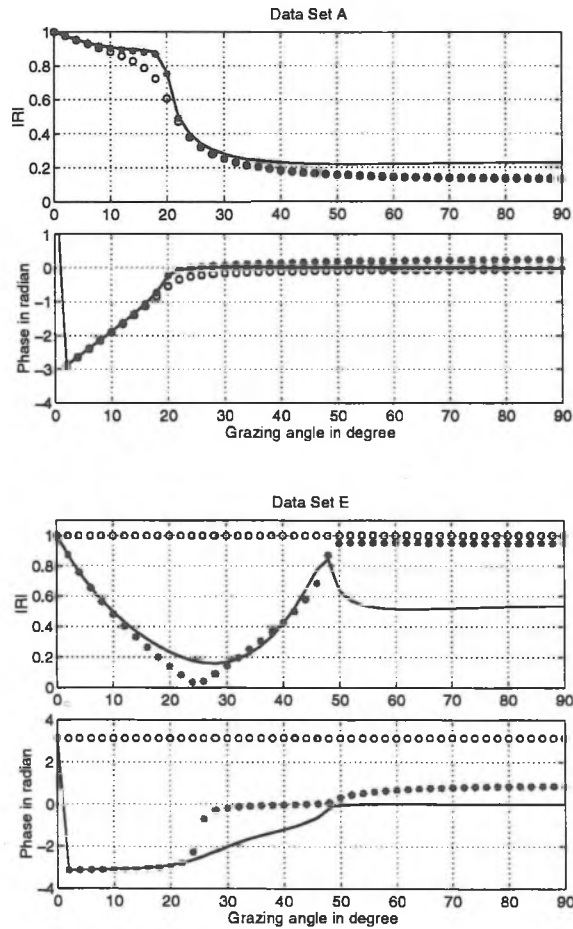

Figure 5 – Reflection coefficient as a function of grazing angle for data sets A and E. (———) solid seabed with shear waves; (○ ○ ○) equivalent fluid with real parameters; (∗ ∗ ∗) equivalent fluid of complex density.

4. DEVELOPMENT OF NEW EFFECTIVE-SEABED MODELS

The object of this section is to develop a new effective-seabed model. First a new equivalent-fluid seabed model is proposed using a relationship between a seabed and its equivalent seabed. Then the angle-dependent parameters of the equivalent-fluid seabed are determined.

4.1 Proposed New Model

Relationship Between Seabeds and Their Equivalent-Fluid Seabeds

The idea associated with the equivalent-fluid seabed is to match the impedance of the 'fluid' with the impedance of the solid seabed. Shear-wave effects will be included in the calculation of the parameters of the 'equivalent fluid'. The reflection coefficient at the fluid/equivalent-fluid interface is obtained by replacing the impedance of the bottom Z_b with that of the equivalent fluid Z_e in Eq. (1):

$$R_{f-ef} = \frac{Z_e - Z_1}{Z_e + Z_1}, \tag{18}$$

with $Z_e = \rho_e \hat{C}_e / \sin\theta_e$, $\sin\theta_e = \sqrt{1 - \hat{C}_e^2 / c^2}$, $\hat{C}_e = c_e/(1 + i\xi\alpha_e)$. ρ_e is termed the effective density, $\hat{C}_e$ is the effective complex sound speed, θ_e is the effective refraction angle, and α_e is the effective attenuation coefficient of the equivalent fluid. Making R_{fs} in Eq. (1) and R_{f-ef} in Eq. (18) equal to one another, we have the relationship for the calculation of the parameters of the equivalent seabed:

$$Z_e = Z_b, \quad \text{ie,} \quad \frac{\rho_e \hat{C}_e}{\sin\theta_e} = \frac{\rho_2 \hat{C}_p P(\theta_1)}{\sin\theta_p}, \tag{19}$$

Snell's law at the fluid/equivalent-fluid seabed interface is:

$$\frac{c_1}{\cos\theta_1} = \frac{\hat{C}_e}{\cos\theta_e}, \tag{20}$$

The parameters – that is, the sound speed, the density and the attenuation coefficient – of the equivalent fluid are determined from Eq. (19). The complex sound speed or the attenuation coefficient of the equivalent-fluid seabed calculated from Eq. (19) should satisfy Snell's law, Eq. (20). The parameters c_e, ρ_e and α_e of the equivalent-fluid seabed can be calculated using Eq. (19). Generally the sound speed of the equivalent fluid c_e is chosen to be equal to the sound speed c_p of the compressional waves in the seabed. The remaining two parameters ρ_e and α_e cannot be uniquely determined by only one equation. Thus Eq. (19) has several solutions for the values ρ_e and α_e. It is noted that Zhang and Tindle's models can be solved from relationship (19) which allows the

impedance of the equivalent fluid Z_e and the total impedance of the seabed to be made equal to one another. In the model with a complex-density equivalent fluid, they choose $c_e = c_p$ and $\alpha_e = \alpha_p$. From Eq. (17), we can obtain $\rho_e = \rho_2 P(\theta_1)$. In this model the refraction angle $\theta_e = \theta_p$, because $\hat{C}_e = \hat{C}_p$. The shear-wave effects in the bottom are represented by the complex density in the equivalent fluid, resulting in energy losses caused by the internal-friction mechanism [11]. However, many existing models may not admit density as a complex quantity, but accept a complex sound speed in the sense that they use a bulk attenuation coefficient for sound waves. For practical purposes, it may be necessary to consider a subset of equivalent-fluid bottoms that have real density values [12]. Eq. (19) is used to develop a new equivalent-fluid seabed model.

Parameters of the equivalent fluid

Focussing on the calculation of the effective impedance of the equivalent-fluid seabed, a new model is derived using Eq. (19).

If the density of the equivalent-fluid seabed is kept equal to its true value, i.e.,:

$$\rho_e = \rho_2, \tag{21}$$

then complex speed of the equivalent-fluid seabed can be solved from Eq. (19):

$$\hat{C}_e = \frac{\hat{C}_p P(\theta_1)}{\sqrt{1 - \hat{C}_p^2 (1 - P^2(\theta_1))/c_1^2}}. \tag{22}$$

The effective impedance of the equivalent-fluid seabed is given by:

$$Z_e = \frac{\rho_e \hat{C}_e}{\sin \theta_e}, \tag{23}$$

where the refraction angle of the equivalent fluid can be calculated using Eq. (20):

$$\sin \theta_e = \sqrt{1 - \hat{C}_e^2/c^2} \tag{24}$$

In this model, unlike the complex-density model [7], the refraction angle in the equivalent fluid is not the same as θ_p. It is noted that the effective refraction angle in the equivalent fluid depends on the shear-wave factor $P(\theta_1)$, the complex compressional-wave speed of the seabed and the sound speed of the fluid, and that it is a function of the grazing angle. It is a complex number. In addition, the number of propagating modes will change as a result of changing the compressional sound speed in the bottom.

The reflection coefficient at the interface of the fluid and the equivalent-fluid seabed is calculated by substituting Z_e into Eq. (18).
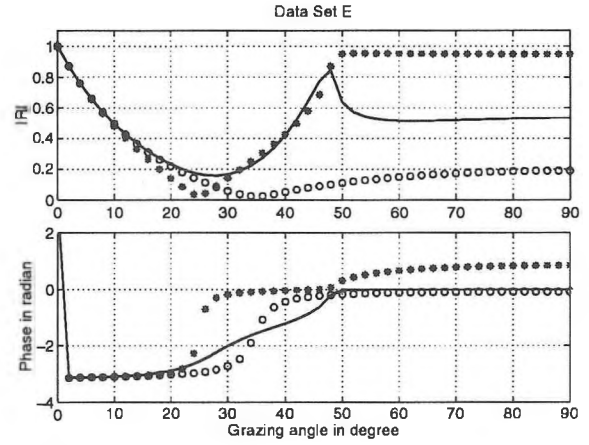

Figure 6 – Reflection coefficient versus grazing angle for data set E. (——) solid seabed with shear attenuations; (o o o) new model of the equivalent-fluid seabed using Eqs. (22) – (24); (∗ ∗ ∗) Tindle and Zhang's complex-density model.

Numerical Evaluation

The reflection coefficient is calculated by Eq. (18). The results are shown in Fig. 6 for data set E. The reflection coefficients of the bottom calculated by Eq. (18) and the results of Zhang and Tindle's complex-density model are also given in Fig. 6 for comparison. It is shown that the reflection coefficient obtained by the new model agrees well with that of the solid bottom at $\theta_1 < 30°$. The new model gives better results than Zhang and Tindle's complex-density model for $10° \leq \theta_1 \leq 28°$. As in practice one is especially interested in low grazing angle, the new model provide better approximation to the solid bottom for large shear-wave speed.

4.2 Effective Seabed with Grazing-Angle-Dependent Parameters

The reason for the error in Zhang and Tindle's model 2, and in the new model, is that the shear factor $P(\theta)|_{\theta_1=0}$ was simply used in the calculation of the parameters of the equivalent seabed. However, this will be good when $|P(\theta) - P(0)| \approx 0$. When c_s is large, $P(\theta)$ is different from $P(0)$. This causes the disagreement between the equivalent fluid and the real seabed. In other words, $P(0)$ cannot represent the effects of the shear waves over a large range of grazing angles. An equivalent fluid of grazing-angle-dependent parameters is proposed therefore to make the equivalent fluids valid at all grazing angles. If $P(0)$ is replaced by $P(\theta_1)$, the grazing-angle-dependent complex density is given as:

$$\rho_e(\theta_1) = \rho_2 P(\theta_1). \tag{25}$$

The reflection coefficient calculated using $\rho_e(\theta_1)$ gives exactly the same values of the reflection coefficient as those of the solid. Generally one is only interested in low grazing angle; however, one can use this new method to correct the errors caused by the use of $P(\theta_1)|_{\theta_1=0}$. Fig. 7 shows an example of such correction, by setting $\theta_1 = 16°$ in $P(\theta_1)$.
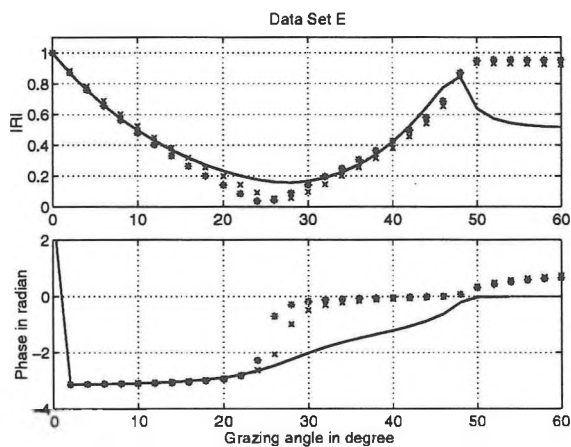
*Figure 7 – Reflection coefficient as a function of grazing angle for data set E. (——) solid seabed with shear waves; (* * *) Tindle and Zhang's complex-density equivalent fluid; (x x x) modified Tindle and Zhang's complex-density equivalent fluid with $\rho_e = \rho_2 P(\theta_1)|_{\theta_1=16°}$.*

5. CONCLUSION

Validations and numerical evaluations of the existing effective seabeds have been made. The validations of the existing effective-seabed models show that the excitation of shear waves in seabeds decreases the amplitude of the reflection coefficients of the fluid/solid interface and its phase shifts. The existence of the shear waves in sea bottoms also decreases the bottom impedance and increases its phase shifts. According to the previous discussions, one could increase the attenuation of the bottom [3, 13] or decrease the impedance of the bottom [4, 5] to match the large bottom losses caused by shear waves.

Tindle and Zhang's first model [6] combines the increase of the attenuation and decrease of the impedance of the bottom. However, when $(c_s/c_1)^2 \approx 0.5$, this model predicts infinite α_s and negative ρ_e. Tindle and Zhang's improved model with complex density [7] gives better agreement with the solid bottom than their original model 1. This model can be used for large shear-wave speed at grazing angles approaching $0°$. When the shear-wave speed becomes larger, this model is valid only at the grazing angle of $0°$. It is possible to extend Zhang and Tindle's second model to very hard seabeds by adjusting the factor $P(\theta_1)$ for calculating the density of the equivalent fluid as shown in Fig. 7.

A new equivalent-fluid seabed model has been developed: the effective impedance of the equivalent-fluid seabed is derived and used in the calculation of the reflection coefficient at the interface of the fluid and the equivalent-fluid seabed. The developed equivalent-fluid seabed model gives better results than the complex-density model [7] for estimation of the reflection coefficient of the seabed at low grazing angles

$\theta_1 < 30°$. For the further work it would be very useful to examine these approximations for a range of realistic sea-bottom types by incorporating them in a propagation model.

REFERENCES

[1] E. L. Hamilton, "Geoacoustic modeling of the sea floor", *J. Acoust. Soc. Am.* **68** (5), 1313-1339 (1980).

[2] H.P. Bucker, "An equivalent bottom for use with the split-step algorithm", *J. Acoust. Soc. Am.* **73** (2), 486-491 (1983).

[3] F.D. Tappert, "Parabolic equation modeling of shear waves", *J. Acoust. Soc. Am.* **78** (5), 1905-1906 (1985).

[4] A.O.J. Williams and R.K. Eby, "Acoustic attenuation in a liquid layer over a slow viscoelastic solid", *J. Acoust. Soc. Am.* **34**, 836-843 (1962).

[5] G.V. Frisk and J.F. Lynch, "Shallow water waveguide characterisation using Hankel transform", *J. Acoust. Soc. Am.* **76**, 205-216 (1984).

[6] C.T. Tindle and Z.Y. Zhang , "An equivalent fluid approximation for a low shear speed ocean bottom", *J. Acoust. Soc. Am.* **91** (6), 3248-3256 (1992).

[7] Z.Y. Zhang and C.T. Tindle, "Improved equivalent fluid approximations for a low shear speed ocean bottom", *J. Acoust. Soc. Am.* **98** (6), 3391-3396 (1995).

[8] David M.F. Chapman and Peter D. Ward, "The normal-mode theory of air-to water sound transmission in the ocean", *J. Acoust. Soc. Am.* **87**(2), 601-618 (1990).

[9] F.B. Jensen and W.A. Kuperman, "Optimum frequency of propagation in shallow water environments", *J. Acoust. Soc. Am.* **73** (3), 813-819 (1983).

[10] L.M. Brekhovskikh and Yu. Lysanov, *Fundamentals of Ocean Acoustics*, 2nd. (Springer-Verlag, Berlin, Germany, 1991).

[11] G. B. Deane, "Internal friction and boundary conditions in lossy fluid seabeds", *J. Acoust. Soc. Am.* **101**(1), 233-240 (1997).

[12] Private Communication with Mr. David Chapman, *Defence Research Establishment Atlantic* on December 2, 1996.

[13] F. Ingenito and S.N. Wolf, "Acoustic propagation in shallow water overlying a consolidated bottom", *J. Acoust. Soc. Am.* **60** (3), 611-617 (1976).

[14] T.W. Tunnel and G.J. Tango , "Predicted partitioning of VLF acoustic energy in a range-dependent environment", in Ocean seismo-acoustics : low-frequency underwater acoustics, edited by Tuncay Akal and Jonathan M. Berkson, J.M. Berkson (Plenum Press, New York, 1986 , pp191-197.

Blachford

"The ABC's of noise control"

H.L. Blachford's Comprehensive Material Choices

Noise treatments can be categorized into three basic elements: Vibration Damping, Sound Absorption and Sound Barriers.

Vibration Damping

It is well known that noise is emitted from vibrating structures or substrates. The amount of noise can be drastically reduced by the application of a layer of a vibration damping compound to the surface. The damping compound causes the vibrational energy to be converted into heat energy. Blachford's superior damping material is called ANTIVIBE and is available either in a liquid or a sheet form.

ANTIVIBE DL is a liquid damping material that can be applied with conventional spray equipment or troweled for smaller/thicker application.

It is water-based, non-toxic and provides economical and highly effective noise reduction from vibration.

ANTIVIBE DS is an effective form of damping material provided in sheet form for direct application to your product.

Sound Barriers

Sound Barriers are uniquely designed for insulating and blocking airborne noise. The reduction in the transmission of sound (transmission loss or "TL") is accomplished by the use of a material possessing such characteristics as high mass, limpness, and impermeability to air flow. Sound barriers can be a very effective and economical method of noise reduction.

Blachford Sound Barrier materials:

BARYMAT

Limp, high specific gravity, plastic sheets or die cut parts. Can be layered with other materials such as acoustical foam, protective and decorative facings to achieve the desired TL for individual applications.

Sound Absorption

Blachford's CONASORB materials provide a maximum reduction of airborne noise through absorption in the frequency ranges associated with most products that produce objectionable noise. Examples: Engine compartments, computer and printer casings, construction equipment, cabs,...etc.

Available with a wide variety of surface treatments for protection or esthetics. Material is available in sheets, rolls and die-cut parts – designed to meet your specific application.

Suggest Specific Material or Design

Working with data supplied by you, H.L. Blachford will make recommendations or treatment methods which may include specific material proposals, design ideas, or modifications to components.

A Quality Supplier

The complete integration of: '

– Experience
– Quality-oriented manufacturing technology
– Research and development
– Problem solving approach to noise control

Our Mississauga Plant is ISO-9001 CERTIFIED

Result in:

Comprehensive Noise Control Solutions